


 Cite this: *RSC Adv.*, 2025, **15**, 36050

Salinity and alkalinity impacts on the interfacial activity of crude oil–water systems using individual and mixtures of a surface-active ionic liquid and conventional surfactant

Simin Asadabadi, * Mona Kharazi and Javad Saien

Surface-active ionic liquids (SAILs) in combination with conventional surfactants offer promising effects on the interfacial properties of crude oil–water systems. Relevantly, aqueous phase salinity and alkalinity exert inevitable impacts. This study explores the impacts of salt and salt–alkali media on the interfacial behavior of a long-chain cationic imidazolium-based SAIL, $[C_{12}\text{mim}][\text{Cl}]$, and the anionic conventional surfactant SDS, individually and in mixtures. Results indicate that SDS alone exhibits higher efficiency, and exposure to salty and/or alkaline media gives rise its activity through a significant reduction in interfacial tension and critical micelle concentration (CMC). Using a surfactant mixture, adaptive charge interactions between surfactants yield synergistic effects in IFT and CMC reductions with optimal performance at a SAIL mole fraction of 0.3. Salt and alkali amplify interfacial activity, resulting in IFT reductions from 26.5 to 1.6 mN m^{-1} with 3.0 wt\% NaCl and further down to 0.2 mN m^{-1} with 3.0 wt\% NaCl and 1.5 wt\% NaOH . Besides, corresponding CMCs dropped substantially, from 9.8×10^{-3} and $9.4 \times 10^{-3}\text{ mol dm}^{-3}$ to 2.3×10^{-3} in a saline medium and $1.5 \times 10^{-3}\text{ mol dm}^{-3}$ in a saline–alkaline medium, respectively. Theoretical analyses, based on the Gibbs adsorption equation and the Rosen model, were employed to evaluate the adsorption characteristics of the individual surfactants and their mixtures, revealing reasonable key parameters that provide deeper insights into basic concepts.

Received 25th August 2025
 Accepted 11th September 2025
 DOI: 10.1039/d5ra06324h
rsc.li/rsc-advances

1. Introduction

Crude oil plays a vital role in driving global economic growth; however, more than 70% of oil reserves remain unrecoverable despite advancements in recovery technologies.¹ Viscous forces and the interfacial tension (IFT) of crude oil and the aqueous phase primarily control the entrapment of oil within porous reservoir rocks. The IFT between crude oil and water is another critical factor limiting oil recovery, especially in mature reservoirs.² To address this challenge, surfactants are employed to reduce IFT. Notably, low IFT values correspond to higher capillary numbers in oil reservoirs,^{3,4} facilitating the mobilization of residual oil through porous media toward production wells as a promising technique for enhanced oil recovery (EOR).⁵

Various surfactants have been investigated in this regard; however, conventional surfactants possess intrinsic limitations because of their sensitivity to media salinity, temperature, and pH.⁶ Consequently, there has been an ongoing effort to create

new materials capable of consistently lowering IFT. In this regard, surface-active ionic liquids (SAILs) have attracted much attention due to their amphiphilic characteristics and robustness under harsh conditions.⁷ SAILs are viewed as promising substances owing to their high activity and desirable attributes, which include stability across extreme temperatures, salinities, and pH ranges, as well as their low toxicity, recyclability, non-flammability, and minimal vapor pressure.^{8,9}

Among different SAIL categories, those based on imidazolium are recognized for their superior activity.³ Nevertheless, the synthesis of SAILs is still in its nascent phase and is recognized as cost-prohibitive.^{10,11} Moreover, to attain effective EORs, substantial reductions in crude oil–water IFT are required. Thus, depending solely on SAILs seems inadequate. To address these issues, research on surfactant mixtures is ongoing. The combination of SAILs with conventional surfactants can produce considerable synergies in IFT reduction, often surpassing the performance of individual surfactants and making them economically viable for EOR. The improved performance stems from the complementary properties of both surfactant types, such as enhanced thermal stability and tunable surface activity. Several studies have highlighted these advantages. In particular, investigations on the (toluene + *n*-decane)–water system have shown extraordinary IFT reductions

Department of Applied Chemistry, Faculty of Chemistry and Petroleum Sciences, Bu-Ali Sina University, Hamedan 6517838695, Iran. E-mail: s.asadabadi@basu.ac.ir; s.asadabadi@gmail.com; m.kharazi@basu.ac.ir; kharazi.mona@yahoo.com; saien@basu.ac.ir; jsaien@yahoo.com; Tel: +98 8131408080



with surfactant mixtures¹² and that blending SAILs with conventional surfactants led to notable enhancements in the interfacial characteristics of crude oil–water systems.^{13,14} Nonetheless, despite the significant progress on blends of SAILs and conventional surfactants, minimal focus has been directed toward the behavior of such mixtures under high-salinity and alkaline conditions in real crude oil systems, which has not been systematically studied. Building upon our earlier works on EOR,^{15,16} this study aims to evaluate the extent of IFT and critical micelle concentration (CMC) reduction in the crude oil–water system under high-salinity and alkaline media, relevant to actual reservoir conditions.

Accordingly, a long-chain cationic imidazolium-based SAIL, 1-dodecyl-3-methylimidazolium chloride, $[C_{12}\text{mim}]^{\text{Cl}^-}$, and the anionic conventional surfactant sodium dodecyl sulfate (SDS), are used here, individually and in a mixture. Synergistic performance offers a cost-effective alternative to relying only on expensive SAILs. Realistic conditions suggest using sodium chloride (NaCl), which is commonly found in seawater and formation brines, and sodium hydroxide (NaOH), which imparts alkaline conditions in brine systems. Alkaline species, like NaOH, naturally increase the alkalinity of formation waters, a condition dominant in carbonate and sandstone reservoirs, and alkaline solutions are used in EOR to mitigate corrosion issues, especially with crude oils with high acid numbers.¹⁷ Experimental data are analyzed with adsorption isotherms to elucidate the mechanisms responsible for observed variations and to determine relevant thermodynamic parameters. The comprehensive scope of this investigation offers valuable

practical knowledge on the application of surfactant mixtures in EOR scenarios under salty and alkaline conditions.

2. Experimental

2.1. Materials

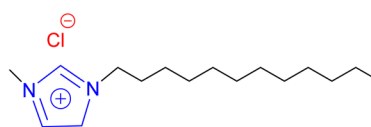
Crude oil specimens were procured from the Marun oil field in southern Iran. The corresponding major specifications/compositions are listed in Table 1. The long-chain cationic imidazolium-based SAIL created for this research features a twelve-carbon alkyl chain with a chlorine anion, which is identified as 1-dodecyl-3-methylimidazolium chloride and denoted as $[C_{12}\text{mim}]^{\text{Cl}^-}$. The synthesis of this SAIL was conducted according to a previously established procedure.¹⁸ The resulting product was confirmed using FTIR, ^1H NMR, ^{13}C NMR, and mass spectrometry. Characterization details and all the relevant spectra are given in the supplementary information. The molecular structures of the imidazolium-based SAIL and the analogous SDS surfactant are shown in Fig. 1. The purity of the synthesized SAIL was determined to be greater than 99.0% based on chloride ion titration. SDS anionic surfactant, sodium chloride salt, NaCl, and sodium hydroxide, NaOH, were purchased from Merck, all with purities exceeding 99.0%. The aqueous phase solutions were prepared with great care using high-purity, freshly deionized water with a conductivity below $0.08 \mu\text{S cm}^{-1}$.

2.2. Instruments and procedure

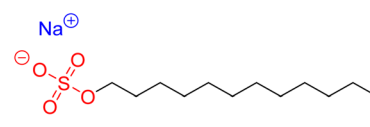
The IFT was measured using a pendant drop tensiometer (model CA-ES10, Fars EOR Technology). In this technique, crude oil was extruded through the tip of a stainless-steel needle, which was immersed in the aqueous bulk phase. The experimental configuration and procedure have been described in detail in a previous publication.¹⁹ IFT values were calculated at different times by assessing the geometric profile of the developing pendant drop and analyzing the images using dedicated software. For each measurement, the pendant drop was monitored until the IFT variation became negligible ($<\pm 0.1 \text{ mN m}^{-1}$). The equilibration time changed depending on the SAIL/surfactant concentration. In crude oil–pure water systems, equilibrium was typically reached after $\sim 20 \text{ min}$, whereas at the highest SAIL/surfactant concentration, it decreased to $\sim 250 \text{ s}$ due to faster adsorption kinetics and enhanced interfacial activity. After equilibrium was achieved, the measurements were continued for an additional period to confirm stability. All IFT tests were repeated under identical conditions (SAIL/surfactant concentration, salinity, and pH) to ensure accuracy.

Table 1 Major specifications/compositions of crude oil

Specifications/compositions	Value
$^{\circ}\text{API}$	20.7
Saturated (wt%)	54.0
Aromatic (wt%)	22.3
Resin (wt%)	6.7
Asphalt (wt%)	7.7
Acidity number (mg KOH per g)	0.09
Sulphur content (wt%)	1.63
Salt content (lbs per 1000 bbls)	4
Water content (wt%)	Nil
Density at 20 °C (g cm ⁻³)	0.915
Viscosity at 70 °F (cP)	55
Viscosity at 100 °F (cP)	44
Kinematic viscosity at 70 °F (cSt)	60
Pour point (°F)	10
Flashpoint (°F)	70
Reid vapor pressure (psi)	12.1
Loss at 200 °C (wt%)	9.3



1-Dodecyl-3-methylimidazolium chloride ($[C_{12}\text{mim}]^{\text{Cl}^-}$), cationic SAIL



Sodium dodecyl sulfate (SDS), anionic surfactant

Fig. 1 Chemical structures of the used SAIL and the SDS conventional surfactant.



and reproducibility. Using this method, an equilibrium IFT of 29.1 mN m^{-1} was established for the crude oil–pure water system, while an IFT of 26.5 mN m^{-1} at 298.2 K was measured for the crude oil–salt water of NaCl (3.0 wt%), approximating the primary salt content in seawater.²⁰ In addition, the surface tension of water (against air) was determined as 71.9 mN m^{-1} at the same temperature, in close agreement with the literature value (72.0 mN m^{-1}).²¹ The experiments were performed under ambient pressure and at a steady temperature of 298.2 K , controlled by a thermostat, with a $\pm 0.1 \text{ K}$ uncertainty.

Prior to the experiments, surfactant solutions were prepared at concentrations ranging from 1.0×10^{-4} to $2.5 \times 10^{-2} \text{ mol dm}^{-3}$ for the individual surfactants and from 1.0×10^{-4} to $2.0 \times 10^{-2} \text{ mol dm}^{-3}$ for the surfactant mixtures, all prepared by mass. Salty solutions of surfactants with NaCl (3.0 wt%, pH 6.8) and in the presence of NaOH (1.5 wt%, pH 9.0) were prepared in the range of (1.0×10^{-4} to $2.5 \times 10^{-2} \text{ mol dm}^{-3}$) for the individual surfactants and (1.0×10^{-4} to $1.0 \times 10^{-2} \text{ mol dm}^{-3}$) for the mixture of surfactants. All solutions were meticulously prepared by mass using an Ohaus digital balance, model AV 264 Adventurer Pro, with an accuracy of $\pm 0.0001 \text{ g}$.

To prepare aqueous solutions, 3.0303 g of NaCl (99.0 wt%) and 1.5151 g NaOH (99.0 wt%) were added to a 100 ml flask containing SAIL and SDS. The composition of the mixtures was adjusted based on the SAIL mole fraction, $\alpha_1 = C_1/C_{12}$, where C_1 denotes the molar bulk concentration of the SAIL, C_2 represents that of the SDS, and $C_{12} = C_1 + C_2$ as the total concentration of the SAIL and SDS in the aqueous phase. For example, with a total concentration of 0.01 mol dm^{-3} and $\alpha_1 = 0.3$, the required amounts of SAIL ($0.01 \times 0.3 = 0.003 \text{ mol dm}^{-3}$) and SDS ($0.01 - 0.003 = 0.007 \text{ mol dm}^{-3}$) were 0.0869 and 0.2039 g, respectively. Accordingly, for the mixture of surfactants, the

SAIL mole fraction (α_1) was varied within the range of 0–1. The density of the solutions, crucial for determining the IFT, was measured using an Anton Paar oscillating densitometer (DMA 4500, Austria) with a density uncertainty of $1.0 \times 10^{-4} \text{ g cm}^{-3}$. CMC was determined as the concentration at the intersection of tangent lines to the upper and lower regions of the IFT variations *versus* the surfactant concentration.

3. Results and discussion

In evaluating surfactant behavior for EOR applications, it is important to simulate reservoir-like conditions since salinity and alkalinity can affect the IFT and CMC *via* surfactant adsorption at the oil–water interface. The corresponding results and analyses of individual surfactants and their mixtures are given below.

3.1. Individual surfactants

Fig. 2 and 3 illustrate the changes in IFT and CMC for individual surfactants under three distinct conditions: pure surfactants, surfactants in a salty aqueous phase of NaCl (3.0 wt%), and surfactants in a salt–alkaline solution containing NaCl (3.0 wt%) and NaOH (1.5 wt%). Notably, each CMC corresponds to the point at which the IFT reaches a plateau, showing no significant decrease despite increasing surfactant concentration.

3.1.1. Salt and alkali free conditions. Fig. 2 demonstrates a significant IFT reduction up to the CMC achieved. In the presence of the individual $[\text{C}_{12}\text{mim}][\text{Cl}]$ and SDS surfactants, the IFT decreases from the initial value of 29.1 mN m^{-1} and 4.0 mN m^{-1} , indicating maximum IFT reductions of 66.5%

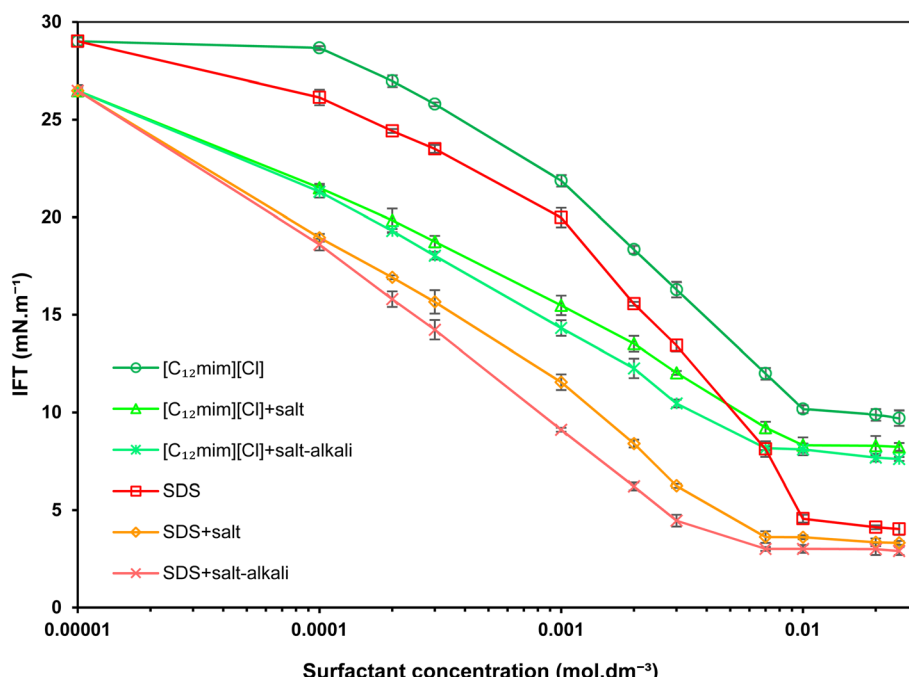


Fig. 2 IFT variation in the crude oil–water system *versus* the concentration of individual surfactants under different conditions.



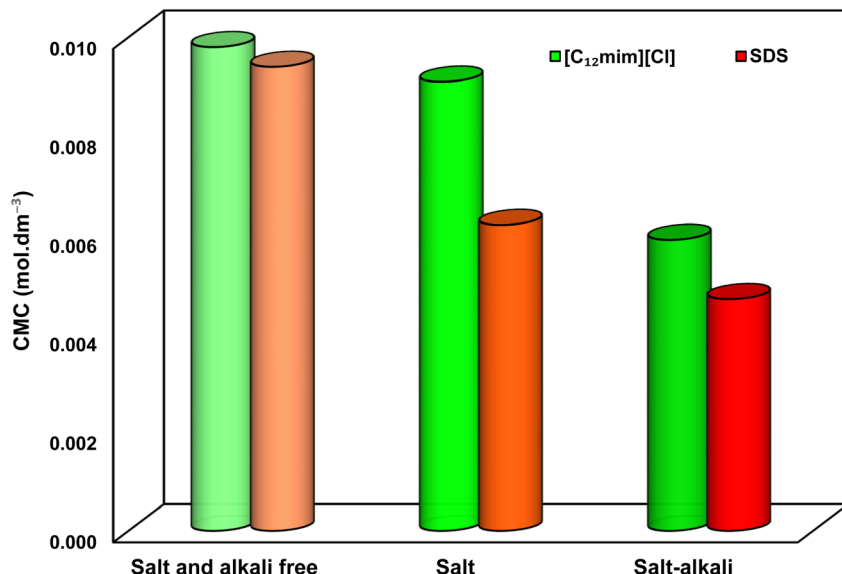


Fig. 3 CMC of individual surfactants under different conditions.

and 86.1%, respectively. Further, as shown in Fig. 3, the corresponding CMCs were 9.8×10^{-3} and 9.4×10^{-3} mol dm⁻³, respectively. These are due to the well-known amphiphilic nature of surfactant molecules. At the interface between crude oil and water, the hydrophobic hydrocarbon tails of the surfactants are oriented in the oil phase, whereas their charged hydrophilic heads are directed toward the aqueous phase.⁹ At concentrations above CMC, the amphiphilic nature compels the surfactants to aggregate, arranging themselves with hydrophobic tails directed inward and hydrophilic heads outward.

3.1.2. Salt condition. The influence of water salinity was examined with a 3.0 wt% NaCl solution, which approximates the primary salt content in seawater. This is important from both operational and economic perspectives, considering the use of seawater and saline solutions for injection into reservoirs.²⁰

As a first point, adding 3.0 wt% of NaCl salt led to an IFT reduction from 29.1 to 26.5 mN m⁻¹ in the absence of surfactants. The potential mechanism behind this effect can be attributed to the accumulation of cations at the interface of the phases. This occurs through a non-covalent interaction of the cations with the hydrocarbon phase, resulting in positive ion adsorption at the interface at low concentrations.²² As a result, even under low salt concentrations in the bulk, the dissociated cations in water tend to localize preferentially at or close to the interface. Consequently, with cations present at the interface, the surface excess increases or becomes positive, leading to a decrease in IFT.²² A second important finding is that the used surfactants were stable in salty water, showing no phase separation or precipitation of surfactants from the solution. In many studies, co-surfactants or co-solvents are added to improve surfactant efficacy and enhance formulation stability in challenging environments, such as salty solutions; however, this approach increases cost and poses potential environmental risks.²³ In contrast, our research achieved stable formulations without the need for co-surfactants or co-solvents.

Fig. 2 shows a significant reduction in IFT with the effect of salt, leading to ultimate IFTs of 8.1 mN m⁻¹ in the presence of [C₁₂mim][Cl] and 3.3 mN m⁻¹ in the presence of SDS. This results in a remarkably greater IFT reduction to 16.3% and 17.6%, respectively, *i.e.* a promising method for EOR applications under challenging salinity conditions. The improved performance observed in the presence of salt can be explained by the following primary mechanisms:

- The counter-charged salt ions diminish the electrostatic repulsion among the surfactant head groups, thereby giving a more compact arrangement of surfactant molecules at the crude oil-water interface.⁹ This tightening of the electrical double layer around the surfactant head groups allows for denser packing of surfactant molecules at the boundaries.^{2,24}
- The salt ions exhibit a high charge density and superior hydration in comparison to surfactant ions, which creates a “salting-out effect” that lowers the solubility of the surfactant in the aqueous phase. As a result, their migration to the interface is enhanced, causing a progressive reduction in IFT in the presence of salt.²⁵

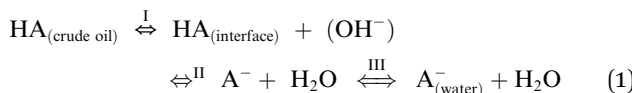
The presence of salt aids in reducing IFT and affects CMC. As shown in Fig. 3, the CMC values for [C₁₂mim][Cl] and SDS fall from 9.8×10^{-3} mol dm⁻³ and 9.4×10^{-3} mol dm⁻³ to 9.1×10^{-3} mol dm⁻³ and 6.2×10^{-3} mol dm⁻³, respectively, corresponding to 7.1% and 34.1% more reductions relative to the salt-free (pure) condition, respectively. Diminishing the electrostatic repulsion between the charged surfactant heads by the counter-charged salt ions results in a compression of the charge layers around the surfactant head groups, which gives closer aggregation in the bulk solution.²⁶ In addition, the salting-out effect accelerates the formation of micelles by lowering the surfactant's solubility in the aqueous phase.

3.1.3. Salt-alkali condition. The effect of salty water containing 3.0 wt% NaCl and 1.5 wt% NaOH was further investigated. The data in Fig. 2 show a more pronounced IFT reduction under alkaline conditions, with IFT values dropping to 7.6 mN



m^{-1} for $[\text{C}_{12}\text{mim}][\text{Cl}]$ and 2.9 mN m^{-1} for SDS. Consequently, the alkaline environment in salty water results in IFT reductions of up to 21.6% and 28.0%, respectively. These observations can be attributed to several phenomena:

- The hydration of sodium ions originating from NaOH gives strong hydration and causes higher migration of surfactant molecules to the interface, enhancing IFT reduction through the salting-out effect.
- It is known that hydroxide ions (OH^-) exhibit a strong tendency to migrate toward the interface.²⁷ By accumulating at the interface, these ions reduce the electrostatic repulsion between the positively charged hydrophilic heads of surfactants, thereby promoting greater interfacial adsorption.
- It has been identified that certain organic acids present in crude oil ($\text{HA}_{(\text{crude oil})}$), like sulfonate and naphthenic acids, can serve as natural surfactants. The acidic groups of these natural surfactants can dissociate at the interface in the presence of hydroxide ions according to the following path,²⁸ leading to the formation of *in situ* surfactants.



An alkaline condition favors dissociation step II in the above path, causing the natural *in situ* surfactants to accumulate more and producing notable reductions in the IFT.²⁸ A schematic diagram of this mechanism is presented in Fig. 4.

The alkaline environment also influences CMC, as demonstrated in Fig. 3, leading to micelle formation at low surfactant concentrations. Under salt-alkali conditions, the CMC values for $[\text{C}_{12}\text{mim}][\text{Cl}]$ and SDS decrease to 5.9×10^{-3} and $4.7 \times 10^{-3} \text{ mol dm}^{-3}$, respectively, representing 39.8% and 50.0% more reductions compared to the non-alkaline salt condition. As pointed out earlier, the salting-out effect reduces the

solubility of surfactants in the aqueous phase, thereby accelerating micelle formation. Additionally, the presence of hydroxide ions (OH^-) lessens the electrostatic repulsion between charged surfactant head groups, facilitating aggregation and promoting efficient micelle formation in the bulk phase.

3.1.4. Theoretical considerations. In order to evaluate the performance of individual surfactants under the applied conditions, crucial parameters related to their interfacial behavior were determined. The γ_{CMC} and γ_{min} , representing, respectively, the IFT at CMC and the minimum achieved IFT, were determined from the variations in IFT *versus* surfactant concentration (Fig. 2). It is worth noting that the absence of a minimum point in the IFT *versus* concentration plot near the CMC indicates the purity of the surfactants.²⁹ Additionally, the effectiveness of IFT reduction, defined as the interfacial pressure at the CMC (Π_{CMC}), can be obtained as follows:³⁰

$$\Pi_{\text{CMC}} = \gamma_0 - \gamma_{\text{CMC}}, \quad (2)$$

where γ_0 denotes the IFT of the pure system without any surface-active additive. Thus, Π_{CMC} serves as a metric for assessing the efficiency of the surfactants relevant to the CMC.⁶

As another important parameter, the maximum interfacial adsorbed concentration, Γ_{max} , reflects the saturation of the interface, beyond which additional surfactant molecules predominantly remain in the bulk phase. Analysis of Γ_{max} can offer insights into molecular packing and interactions at the interface. High values of Γ_{max} indicate dense molecular packing, which often correlates with enhanced interfacial activity and stronger synergistic effects in mixed surfactant systems. Conversely, lower values suggest either weaker adsorption or repulsive interactions that limit surface coverage.

By utilizing the Gibbs adsorption equation, which provides a fundamental thermodynamic relationship linking the surface concentration of adsorbed molecules to the variation of IFT

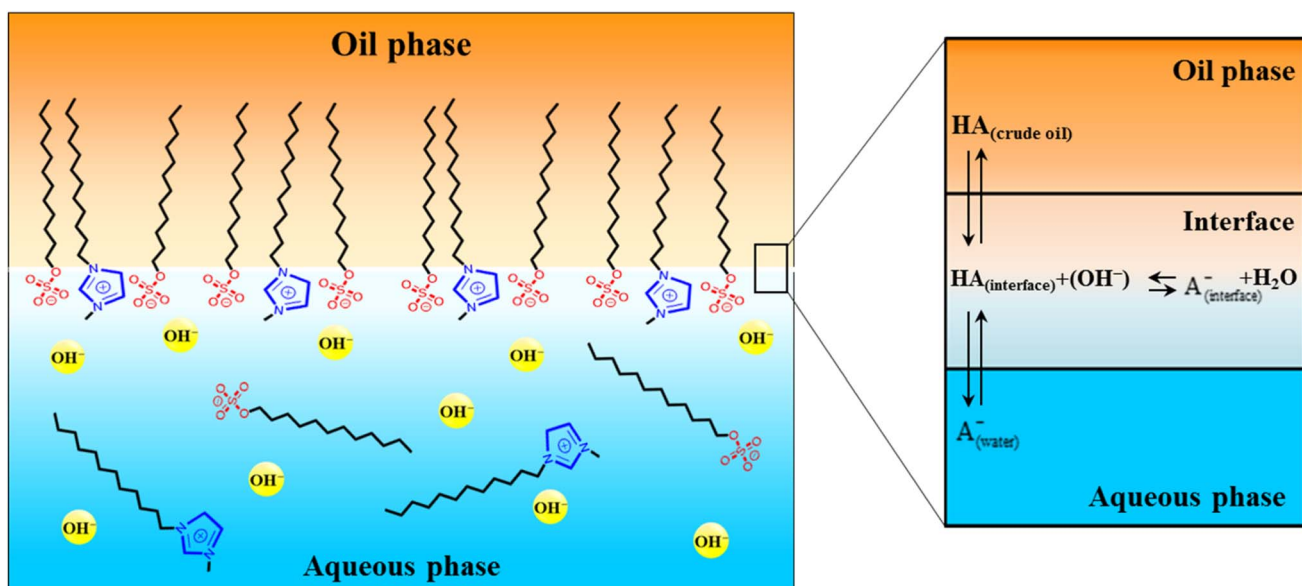


Fig. 4 Schematic of the creation of natural *in situ* surfactants at the crude oil–water interface under alkaline conditions.



with bulk concentration, Γ_{\max} can be calculated using the following equation:³¹

$$\Gamma_{\max} = -\frac{1}{iRT} \left(\frac{d\gamma}{d \ln C} \right), \quad (3)$$

where γ , R , T , and C represent the IFT, the ideal gas constant, the absolute temperature, and the adsorbate concentration, respectively. The parameter i signifies the number of surfactant species. Since the surfactants utilized in this study dissociate into a cation and an anion, the value of i is equal to 2.⁶

Subsequently, the minimum interface area occupied by each molecule, A_{\min} , can be determined as follows:

$$A_{\min} = \frac{1}{N_{\text{Av}} \Gamma_{\max}}, \quad (4)$$

where N_{Av} denotes Avogadro's number. Furthermore, the tendency for micellization can be evaluated through the free energy of micellization, ΔG_m , expressed as follows:³²

$$\Delta G_m = RT \ln(\text{CMC}). \quad (5)$$

Moreover, the standard free energy of adsorption (ΔG_{ads}), indicating the spontaneity of the surfactant adsorption at the interface, is calculated as follows:³¹

$$\Delta G_{\text{ads}} = \Delta G_m - \frac{\Pi_{\text{CMC}}}{\Gamma_{\max}} \quad (6)$$

By applying these equations, the calculated parameters for the individual surfactants in three states (salt and alkali free, salt water, and salt-alkali water) are listed in Table 2.

The results show that the effectiveness of SDS in lowering IFT is greater than that of the imidazolium-based SAIL. Furthermore, the inclusion of salt and alkali boosts the performance of both surfactants, resulting in additional IFT reductions. Consequently, in the three experimental scenarios, the imidazolium-based SAIL attains a maximum IFT reduction of about 66.5%, 69.3%, and 71.3%, whereas SDS shows impressive maximum IFT reductions of 86.1%, 87.5%, and 88.8%. This discrepancy is likely due to the bulkier structure

and larger spatial requirement of the imidazolium SAIL, caused by its aromatic ring, which leads to a lower concentration of adsorbed SAIL molecules at the interface compared to SDS, and thus a smaller reduction in IFT. The interfacial pressure criterion, Π_{CMC} , indicates higher values for SDS, aligning with SDS's greater adsorption tendency.

Accordingly, the higher values of Γ_{\max} for SDS in comparison to the SAIL under all the conditions validate the higher interfacial concentration of SDS, which adopts a more tightly packed arrangement at the interface, leading to a smaller interfacial area per adsorbed molecule (A_{\min}) compared to the imidazolium-based SAIL. They also revealed the beneficial effects of salt and alkali on the adsorption of both surfactants at the interface, confirming their adsorption tendency and promoting a more compact orientation.

Comparing the CMCs in Table 2, low CMCs are observed for both surfactants owing to their significant hydrophobicity. The comparable CMC values of $[\text{C}_{12}\text{mim}][\text{Cl}]$ and SDS in the salt and alkali free system underscore their similar hydrophobic characteristics. However, the CMC reduction for the SAIL caused by salt water and salt-alkali water conditions, with the maximum synergy of 39.8% is less than that of SDS, which exhibits up to a 50.0% reduction.

Finally, the negative values of the associated Gibbs free energies confirm the shared tendency of both surfactants to adsorb at the interface and to form micelles spontaneously, being more significant for SDS under all the three conditions. The absolute values of ΔG_{ads} compared to ΔG_m indicate that surfactant adsorption at the interface takes precedence over micellization for both surfactants.³¹ The presence of salt and alkali enhances these processes, making them more negative and, hence, more spontaneous.

3.2. Mixture of surfactants

In the next step of this study, the influence of salinity and alkalinity on the behavior of SAIL and surfactant mixtures is examined. Fig. 5 illustrates the changes in IFT as a function of mixture concentration for different SAIL mole fractions (α_1) under both the salt and salt-alkali conditions.

Table 2 Interfacial parameters for the individual surfactants

Parameter	[C ₁₂ mim][Cl]			SDS		
	Salt and alkali free	Salt	Salt-alkali	Salt and alkali free	Salt	Salt-alkali
Pure IFT (mN m ⁻¹)	29.1	26.5	26.5	29.1	26.5	26.5
γ_{\min} (mN m ⁻¹)	9.7	8.1	7.6	4.0	3.3	2.9
Max IFT reduction (%)	66.5	69.3	71.3	86.1	87.5	88.8
IFT reduction (%)	—	16.3	21.6	—	17.6	28.0
CMC $\times 10^3$ (mol dm ⁻³)	9.8	9.1	5.9	9.4	6.2	4.7
CMC reduction (%)	—	7.1	39.8	—	34.1	50.0
γ_{CMC} (mN m ⁻¹)	10.4	8.9	8.3	4.7	4.1	4.0
Π_{CMC} (mN m ⁻¹)	18.6	17.6	18.2	24.3	22.4	22.5
$\Gamma_{\max} \times 10^5$ (mol m ⁻²)	55.1	60.5	61.1	71.4	74.3	75.9
$A_{\min} \times 10^2$ (nm ²)	29.2	26.6	26.3	22.5	21.6	21.2
ΔG_m (kJ mol ⁻¹)	-11.4	-11.6	-12.7	-11.5	-12.6	-13.2
ΔG_{ads} (kJ mol ⁻¹)	-11.5	-11.7	-12.8	-11.6	-12.7	-13.3



3.2.1. Salt and alkali free conditions. Fig. 5 shows that there is a consistent decrease in IFT as the surfactant concentration rises for all the mole fractions under salt and salt–alkali conditions. The ease of adsorption at low concentrations leads to a more pronounced slope in the IFT variation. The inset graph emphasizes the changes in IFT in relation to the SAIL mole fraction (α_1) at various mixture concentrations, revealing a marked reduction in IFT with α_1 before increasing toward the

SAIL alone. Hence, under both the established conditions, the minimum IFT value appears at the SAIL mole fraction of $\alpha_1 = 0.3$.

Here, the degree of synergy can be determined by comparing the IFT achieved with the linear combination of the SAIL and SDS contributions in the mixtures (*i.e.* assuming no synergism) at a given concentration:

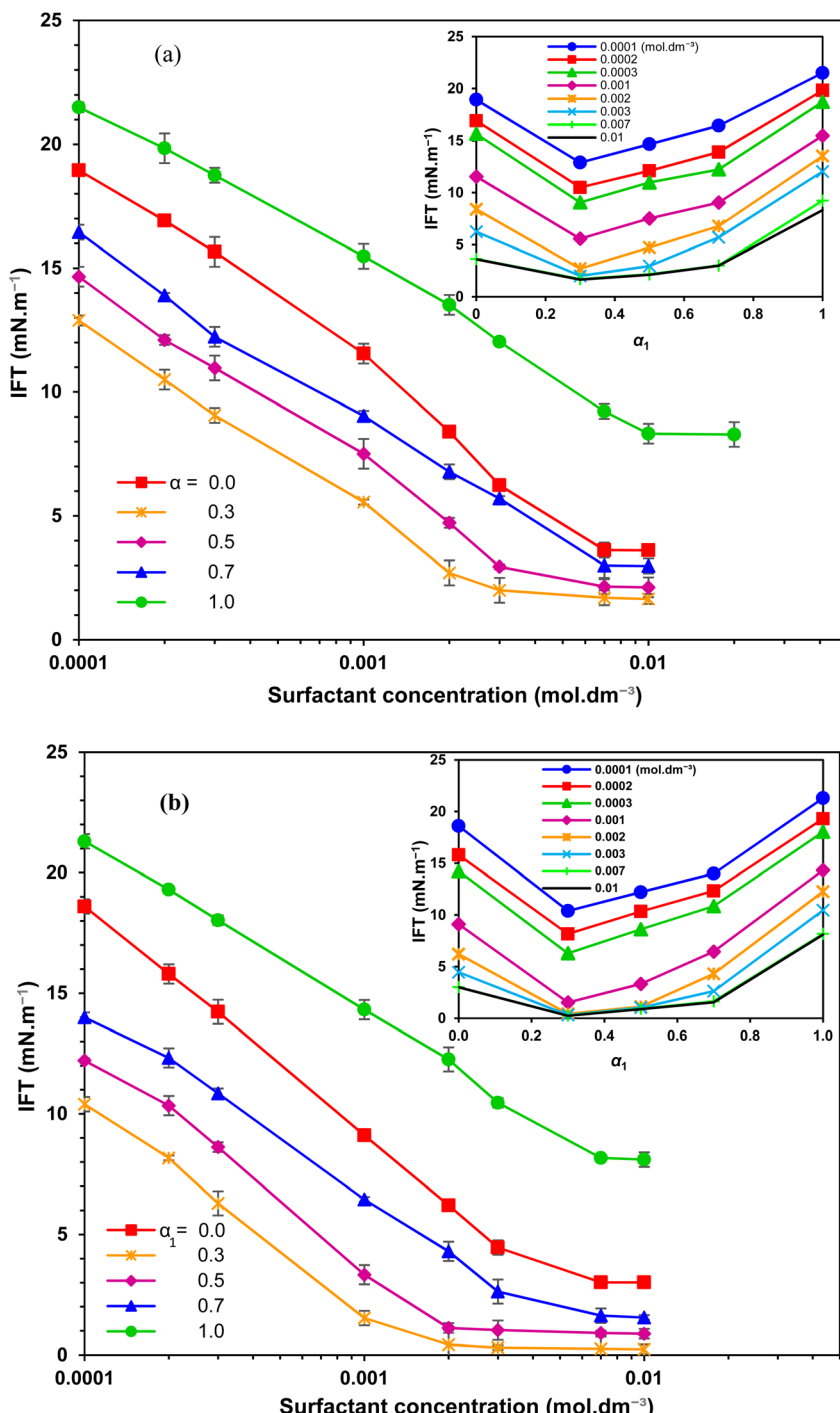


Fig. 5 Variation in the crude oil–water IFT versus the concentration of surfactants for different mole fractions under (a) salt and (b) salt–alkali conditions. The inset figures show the IFT changes versus α_1 at different mixture concentrations.



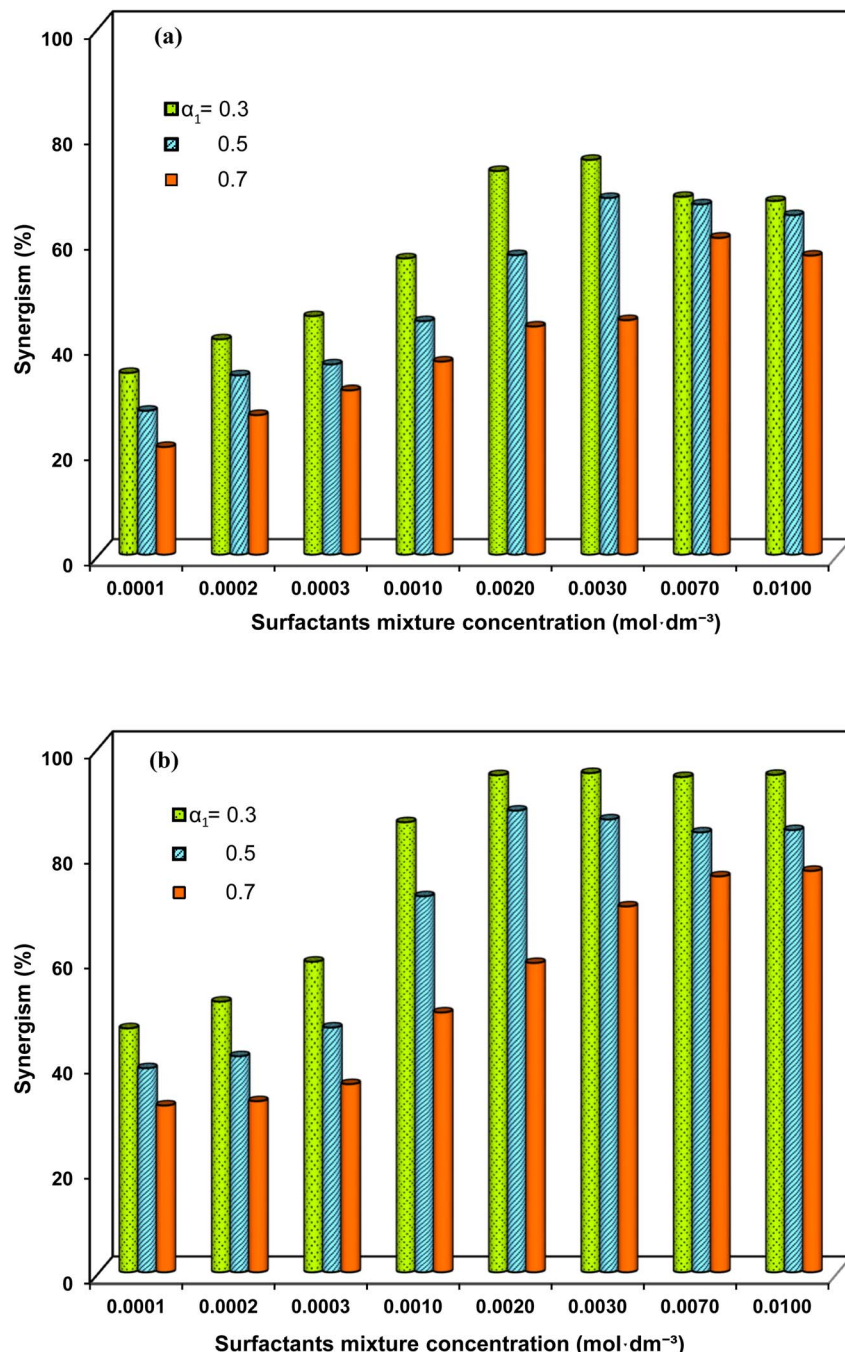


Fig. 6 Synergy percentage in IFT reduction *versus* the concentration of the mixture of surfactants for different mole fractions under (a) salt and (b) salt–alkali conditions.

$$\text{Synergy (\%)} = \left(1 - \frac{\gamma_{\text{mix}}}{\alpha_1 \gamma_{\text{SAIL}} + \gamma_{\text{SDS}}} \right) \times 100, \quad (7)$$

where γ_{mix} , γ_{SAIL} and γ_{SDS} denote the IFT with the mixture, with only the SAIL, and just with SDS, respectively.

Accordingly, the percentage of synergy in IFT reduction *versus* mixture concentration for different α_1 values is illustrated in Fig. 6, with both the salty and salt–alkaline waters. The trend of changing the percentage of synergy with the mixture concentration remains consistent with α_1 ; however, the figure

shows a significant rise at low concentrations, peaking, and then staying relatively constant with slight decreases at high concentrations. This is due to the neutralization of electrostatic repulsion when positively and negatively charged molecules are in close proximity at low concentrations, resulting in high synergisms. At high concentrations, the tight packing of adsorbed molecules causes minor changes in the synergy level. The highest degree of synergy of 74.9% and 95.0% corresponds to salt water and salt–alkali conditions, with a SAIL mole fraction of $\alpha_1 = 0.3$ and a mixture concentration of $0.003 \text{ mol dm}^{-3}$.

From an economic viewpoint, these achievements must have a low SAIL mole fraction. Indeed, a bulky SAIL head group and the charge distribution in the aromatic ring facilitate the attraction of two SDS molecules alongside each SAIL molecule, contributing to the observed synergy.³³ Notably, the findings from this study show a considerably greater level of synergy than those reported in earlier studies on mixtures of cationic and anionic surfactants^{34,35} as well as SAILS with conventional surfactants.^{15,36}

However, the variations in the CMC of the mixtures and γ_{CMC} values across different SAIL mole fractions (α_1) are depicted in Fig. 7 under different conditions. Under all the studied conditions, the CMC decreases to remarkably low values at all mole fractions, with the strongest effect appearing at $\alpha_1 = 0.3$

(Fig. 7a). Consistent with previous findings, the intermolecular attractive forces between surfactants weaken electrostatic repulsion, facilitating micelle formation at lower concentrations. It has to be emphasized that a low CMC is crucial in EOR processes for the efficient transportation of oil droplets through surfactant flooding.^{37,38} Further, comparing γ_{CMC} values for different SAIL mole fractions (Fig. 7b) reveals that in addition to CMC, the relevant IFTs also decrease in the presence of the mixture of surfactants.

To provide a more precise comparison of the results obtained in this study with previous investigations, Table 3 presents interfacial parameters for mixtures of SAIL/surfactant in water-crude oil systems. As shown, compared to other studies,^{39–42} the present study demonstrates outstanding

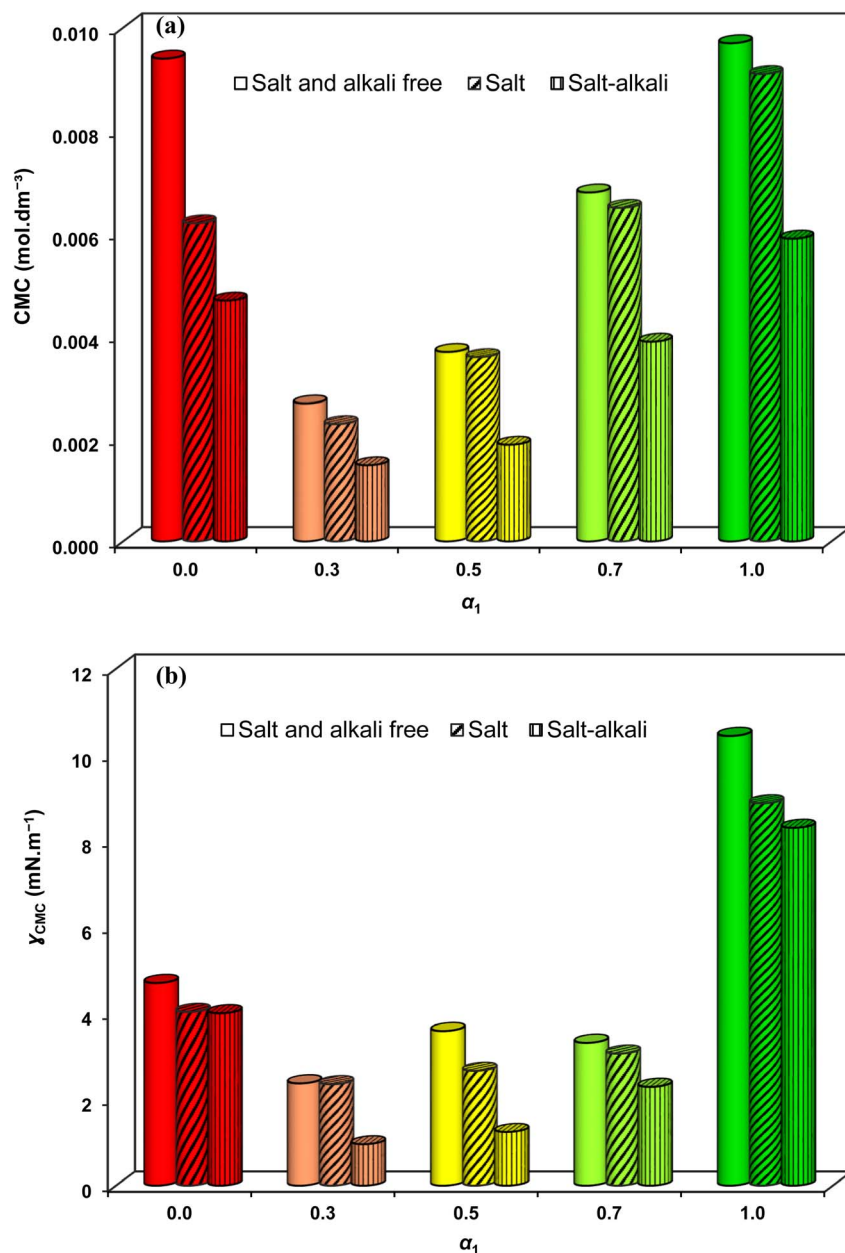


Fig. 7 Variations in (a) CMC and (b) γ_{CMC} versus SAIL mole fraction under different conditions.



Table 3 Comparison of the results with other related studies under salt and alkali free conditions

Crude oil source, type	Used SAIL	T (°C)	α_1	C_{12} (mol dm ⁻³)	Max. γ reduction (%) than the sole SAIL	γ_{CMC} reduction (%) than the sole SAIL	Ref.
Ankleshwar (India), light	1-Hexadecyl-3-methyl imidazolium bromide	35	0.80	0.220	2	50	39
Karamay (China), heavy	1-Dodecyl-3-methylimidazolium chloride	30	0.33	0.017	86	27	40
Tapis (China), light	Choline laurate	25	0.60	0.219	72	—	41
Arab (Saudi Arabia), light	1-Butyl-3-methylimidazolium lauroyl sarcosinate	25	0.83	0.177	46	—	42
Marun (Iran), heavy	1-Dodecyl-3-methylimidazolium chloride	25	0.30	0.003	86	77	15

performance. Using a total concentration of only 0.003 mol dm⁻³ and a low SAIL mole fraction of 0.3 at 25 °C, significant reductions in both IFT and γ_{CMC} were achieved compared to the sole SAIL, highlighting the superior performance of the present study under mild conditions.

3.2.2. Salty condition. The influence of water salinity on the surfactant mixture was examined using a 3.0 wt% NaCl solution. In a manner similar to the individual surfactants, the mixture of the surfactants was found to be stable in salt systems, with no signs of phase separation or precipitation, and without the need for any co-solvents to enhance formulation stability in challenging environments.

The results illustrated in Fig. 5a indicate a significant reduction in IFT by the addition of the salt, leading to an IFT decrease of up to 1.6 mN m⁻¹ with the SAIL mole fraction of $\alpha_1 = 0.3$. The inclusion of salt demonstrates a synergistic influence on IFT reduction in the mixture, achieving up to 74.9% synergy compared to the linear contribution of the surfactants in the salt and alkali free system, as shown in Fig. 6a. For comparison, the related interfacial parameters for the surfactant mixture under various conditions are compiled in Table 4. Analogous to the individual surfactants, the improved performance in the presence of salt is attributed to the salting-out effect and the compression of the electrical double layer around the surfactant head groups, which is due to the counter-charged ions from the salt. These factors promote a more compact arrangement of the surfactant molecules at the interface, leading to a greater IFT reduction with salt.

The addition of salt not only leads to a further reduction in IFT but also impacts the CMC and γ_{CMC} (Fig. 7). The results indicate micelle formation at lower concentrations of the surfactant mixture, while the corresponding IFTs are significantly reduced. In the presence of salt, the CMC decreases to a very low value of 2.3×10^{-3} mol dm⁻³ at $\alpha_1 = 0.3$, representing a 14.8% reduction compared to the salt-free condition. The presence of counter-charged ions in the salt lessens the electrostatic repulsion between the charged heads of the surfactants, leading to a compression of the charge layers surrounding the surfactant head groups and promoting the aggregation of surfactants in the bulk solution.²⁶ The low IFT value of 2.4 mN m⁻¹, achieved at this CMC, highlights the superior performance of the surfactant mixture under salt conditions.

3.2.3. Salt-alkali system. The combined effects of salt and alkali on the reduction of IFT and CMC were examined using a solution containing 3.0 wt% salt and 1.5 wt% NaOH, respectively. The alkali environment in the salt water leads to a more significant reduction in IFT with the surfactant mixture. This caused IFT to reach an exceptionally low value of 0.2 mN m⁻¹ at the SAIL mole fraction of $\alpha_1 = 0.3$ (Fig. 5b). The salt-alkali solution creates a synergistic effect on IFT reduction with the surfactant mixture, reaching up to 95.0% compared to the linear contribution of the surfactants in the salt and alkali free system (Fig. 6b). Fig. 8 better demonstrates that the maximum synergism (under SAIL mole fraction of $\alpha_1 = 0.3$), under salt-alkali conditions, exceeds those under salt conditions across all the mixture concentrations.

The enhanced performance of the surfactant mixture under salt-alkaline conditions aligns with the mechanisms described for individual surfactants in Subsubsection 3.1.3. For better visualization, Fig. 9 illustrates the most likely arrangement of surfactant molecules in the mixture at the oil–water interface under different conditions.

The alkaline condition also affects CMC and γ_{CMC} (Fig. 7), resulting in micelle formation at lower concentrations of the surfactant mixture and correspondingly lower IFTs at the CMC. In this system, the CMC decreases to a very low value of 1.5×10^{-3} mol dm⁻³ at $\alpha_1 = 0.3$, providing 44.4% and 38.8% lower values compared to the salt and alkali free (pure) and only salt conditions, respectively. The salting-out effect aids micelle formation by decreasing surfactant solubility in the aqueous

Table 4 Corresponding parameters for the mixture of surfactants under different conditions

Parameter	Salt and alkali free	Salt	Salt-alkali
Pure IFT (mN m ⁻¹)	29.1	26.5	26.5
γ_{min} (mN m ⁻¹)	1.8	1.6	0.2
Max IFT reduction (%)	93.8	94.0	99.2
Max synergy of IFT reduction (%)	83.6	74.9	95.0
Min CMC $\times 10^3$ (mol dm ⁻³)	2.7	2.3	1.5
Max synergy of CMC reduction (%)	71.5	67.5	70.4
Min γ_{CMC} (mN m ⁻¹)	2.41	2.39	0.98



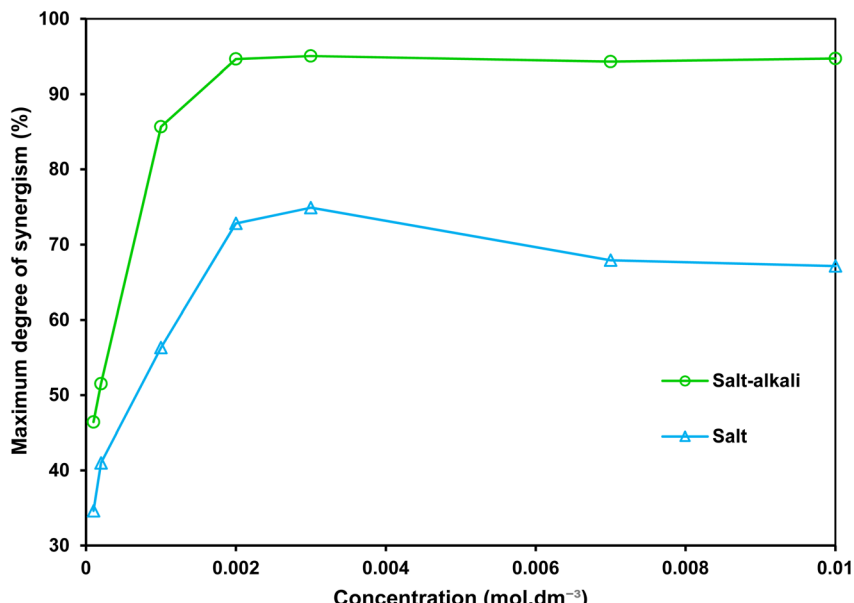


Fig. 8 The maximum degree of synergism against the surfactant mixture concentration under salt and salt–alkali conditions, all with the SAIL mole fraction of $\alpha_1 = 0.3$.

phase. Additionally, hydroxide ions reduce the electrostatic repulsion between the charged heads of the surfactants, facilitating a closer arrangement and promoting aggregation of the surfactants in the bulk. Accordingly, the very low IFT of 0.98 mN m^{-1} signifies the optimal performance of the surfactant mixture under salt–alkali conditions.

3.2.4. Theoretical considerations. The non-ideal binary mixture (NIBM) theory⁶ was applied to analyze the results with the mixture of surfactants and to obtain the adsorbed SAIL mole fraction (X_1) and the molecular interaction parameter (β) using the following equations:⁶

$$\frac{(X_1)^2 \ln(C_{12}\alpha_1/C_1^0 X_1)}{(1-X_1)^2 \ln[C_{12}(1-\alpha_1)/C_2^0(1-X_1)]} = 1, \quad (8)$$

$$\beta = \frac{\ln(C_{12}\alpha_1/C_1^0 X_1)}{(1-X_1)^2}. \quad (9)$$

Here, C_1^0 , C_2^0 and C_{12} represent the bulk concentration of the SAIL, SDS, and their mixture, respectively, all corresponding to a specific IFT. These concentrations were derived from IFT variations *versus* individual surfactant concentrations and their mixture for a particular α_1 value (Fig. 5). The same procedure was employed in our previous studies.^{15,16} Consequently, accurate values of X_1 and β were calculated using an iterative method based on eqn (8) and (9).⁶ Negative values of β indicate an attractive molecular interaction, while positive values represent repulsion.

It is evident from Fig. 10a and b that the adsorbed SAIL mole fraction (X_1) in salty water and salt–alkali water increases with a rise in the mole fraction of SAIL (α_1) under both the salt and salt–alkali conditions. The results also show that as the interfacial concentration increases and the IFT decreases, X_1 decreases, suggesting that SDS has a higher affinity for interfacial adsorption compared to the imidazolium-based SAIL.

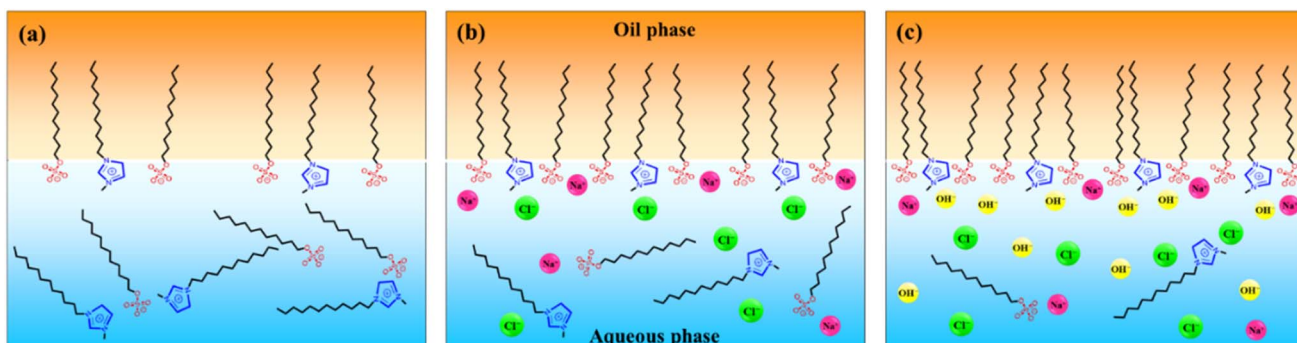


Fig. 9 Orientations of the SAIL and SDS molecules at the crude oil–water interface under (a) salt and alkali free, (b) salt, and (c) salt–alkali conditions.



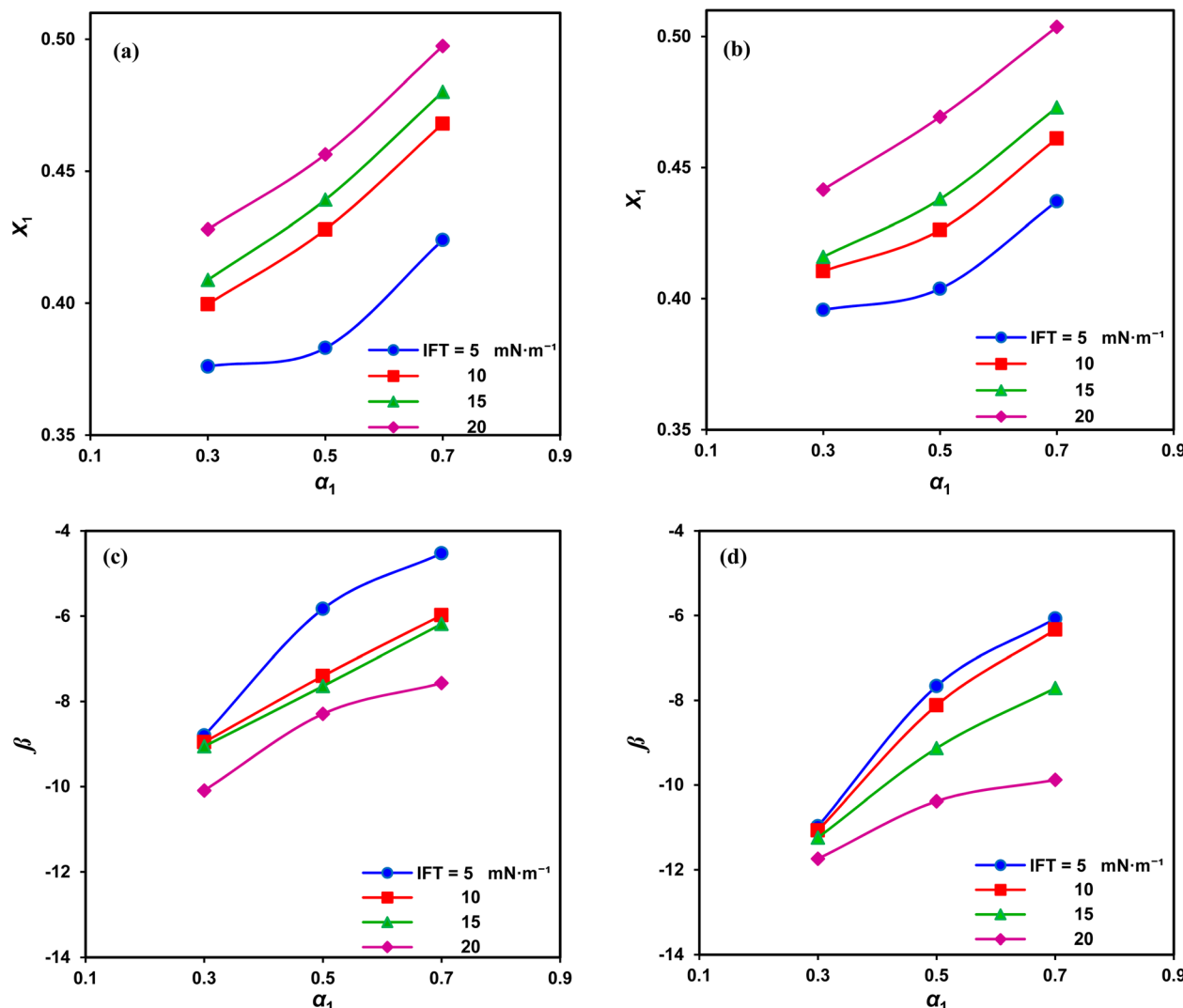


Fig. 10 Interface mole fraction under (a) salty water and in (b) salt–alkali conditions, and interaction parameter under (c) salty water and under (d) salt–alkali water conditions versus the SAIL mole fraction for various constant IFT values.

Comparing the salt and salt-alkali conditions indicates that the alkali addition gives rise to X_1 across all mole fractions, confirming that alkali enhances interfacial adsorption, as elaborated in the previous sections.

The interaction parameter (β) represents the strength and nature of the interactions between surfactant molecules at the interface. A positive β indicates repulsive interactions, while a negative one indicates attractive interactions. By analyzing β , one can gain insight into the molecular organization and interactions occurring at the interface. As shown in Fig. 10c and d, the negative values of β signify an attractive interaction prevailing between the adsorbed components in the mixtures under both the salty water and salt-alkali conditions despite self-repulsions among individual surfactant molecules. Additionally, the relatively high absolute β values imply a strong synergistic effect.⁴³ The highest absolute interaction is observed at $\alpha_1 = 0.3$. Further, the absolute β values decrease as the IFT decreases. This is attributed to the higher interfacial

concentrations and closer arrangement of the adsorbed surfactant molecules, intensifying repulsion between similar charged molecules. Alkaline conditions enhance the absolute value of β , consistent with greater synergism. Hydroxide ions also contribute to the reduction of electrostatic repulsion between like-charge species, favoring attraction between the SAIL and SDS and ultimately achieving a higher IFT reduction.

4. Conclusions

This investigation explored the effects of salty and salt-alkali waters on the interfacial activity of crude oil–water using individual and mixtures of a long-chain cationic SAIL and the anionic conventional surfactant. Preliminary experiments on the individual surfactants confirmed that SDS achieved a stronger reduction in IFT than SAIL. This study also uncovered the synergy in the individual surfactant systems when exposed to salty and salt-alkali waters, which resulted in a greater IFT

reduction than in the salty and alkali free (pure) systems. The salting-out effect and the lessening of electrostatic repulsion between like-charged surfactants in the presence of salt and alkali were identified as primary factors that boosted surfactant interfacial activity. Furthermore, under alkaline conditions, the generation of *in situ* surfactants from natural compounds in the crude oil contributes to the IFT reduction. To provide a thorough evaluation of the effectiveness of individual surfactants, several theoretical parameters were obtained, illustrating the influence of salt and salt-alkali on each parameter.

The synergistic behavior in the surfactant mixtures resulted in a substantial decrease in IFT that surpassed the capabilities of the individual components. The optimal performance was found at a SAIL mole fraction of 0.3, which yielded exceptionally low IFT values. In addition, the CMC was lowered to minimal values. The presence of salt and alkali greatly improved the interfacial activity of the surfactant mixtures, causing further reductions in IFT and CMC. The lowest IFT values achieved with salt and salt-alkali were as low as 1.6 and 0.2 mN m⁻¹, respectively. These IFT changes were consistent with the NIBM model, and the theoretical parameters showed reasonable correspondence.

To accomplish this research, further studies should focus on establishing more realistic reservoir conditions, *e.g.* high pressures and temperatures as well as core flooding tests. Alternative crude oil samples are also viable to examine.

Author contributions

Simin Asadabdi: experiments, methodology, visualization, software, data curation, original draft preparation, writing-review and editing. Mona Kharazi: visualization, investigation, writing initial draft. Javad Saien: methodology, funding acquisition, formal analysis, writing-review and editing.

Conflicts of interest

There are no conflicts of interest to declare.

Data availability

The data supporting this article have been included as part of the supplementary information (SI). Supplementary information is available. See DOI: <https://doi.org/10.1039/d5ra06324h>.

Acknowledgements

Financial support by the authorities of Bu-Ali Sina University is highly acknowledged.

References

- 1 E. Tamayo-Mas, H. Mustapha and R. Dimitrakopoulos, Testing geological heterogeneity representations for enhanced oil recovery techniques, *J. Pet. Sci. Eng.*, 2016, **146**, 222–240, DOI: [10.1016/j.petrol.2016.04.027](https://doi.org/10.1016/j.petrol.2016.04.027).
- 2 N. Pal, N. Saxena and A. Mandal, Studies on the physicochemical properties of synthesized tailor-made gemini surfactants for application in enhanced oil recovery, *J. Mol. Liq.*, 2018, **258**, 211–224, DOI: [10.1016/j.molliq.2018.03.037](https://doi.org/10.1016/j.molliq.2018.03.037).
- 3 P. Pillai, A. Kumar and A. Mandal, Mechanistic studies of enhanced oil recovery by imidazolium-based ionic liquids as novel surfactants, *J. Ind. Eng. Chem.*, 2018, **63**, 262–274, DOI: [10.1016/j.jiec.2018.02.024](https://doi.org/10.1016/j.jiec.2018.02.024).
- 4 L. Zhang, Y. Geng, W. Duan, D. Wang, M. Fu and X. Wang, Ionic liquid-based ultrasound-assisted extraction of fangchinoline and tetrandrine from *Stephaniae tetrandrae*, *J. Sep. Sci.*, 2009, **32**, 3550–3554, DOI: [10.1002/jssc.200900413](https://doi.org/10.1002/jssc.200900413).
- 5 M. Kharazi and J. Saien, in *Surfactants-Fundamental Concepts and Emerging Perspectives*, IntechOpen, 2024, pp. 87–117, DOI: [10.5772/intechopen.112762](https://doi.org/10.5772/intechopen.112762).
- 6 M. J. Rosen, *Surfactants and Interfacial Phenomena*, Wiley, 3rd edn, 2012.
- 7 M. Kharazi, J. Saien, A. Javadi and R. Miller, *Innovations in Ionic Liquid-Based Surfactants and Interfacial Phenomena*, CRC Press, Boca Raton, 2025, ISBN: 9781032748078.
- 8 M. Kharazi, J. Saien, M. Yarie and M. A. Zolfigol, Promoting activity of gemini ionic liquids surfactant at the interface of crude oil-water, *Pet. Res.*, 2021, **117**, 113–123, DOI: [10.1021/jp9804345](https://doi.org/10.1021/jp9804345).
- 9 J. Saien, M. Kharazi, V. Pino and I. Pacheco-Fernández, Trends offered by ionic liquid-based surfactants: applications in stabilization, separation processes, and within the petroleum industry, *Sep. Purif. Rev.*, 2023, **52**, 164–192, DOI: [10.1080/15422119.2022.2052094](https://doi.org/10.1080/15422119.2022.2052094).
- 10 O. Lebedeva, D. Kultin, A. Zakharov and L. Kustov, Advances in application of ionic liquids: fabrication of surface nanoscale oxide structures by anodization of metals and alloys, *Surf. Interfaces*, 2022, **34**, 102345, DOI: [10.1016/j.surfin.2022.102345](https://doi.org/10.1016/j.surfin.2022.102345).
- 11 J. Saien, M. Kharazi, B. Shokri, M. Torabi and M. A. Zolfigol, A comparative study on the design and application of new nano benzimidazolium gemini ionic liquids for curing interfacial properties of the crude oil-water system, *RSC Adv.*, 2023, **13**, 15747–15761, DOI: [10.1039/d3ra01783d](https://doi.org/10.1039/d3ra01783d).
- 12 H. Jia, X. Leng, M. Hu, Y. Song, H. Wu, P. Lian, Y. Liang, Y. Zhu, J. Liu and H. Zhou, Systematic investigation of the effects of mixed cationic/anionic surfactants on the interfacial tension of a water/model oil system and their application to enhance crude oil recovery, *Colloids Surf. A*, 2017, **529**, 621–627, DOI: [10.1016/j.colsurfa.2017.06.055](https://doi.org/10.1016/j.colsurfa.2017.06.055).
- 13 J. Saien, A. Eghitenaei and M. Kharazi, Synergistic performance of a Gemini nano ionic liquid and sodium dodecyl sulfate surfactants at the crude oil-water interface, *Arab. J. Chem.*, 2023, **16**, 105329, DOI: [10.1016/j.arabjc.2023.105329](https://doi.org/10.1016/j.arabjc.2023.105329).
- 14 J. Saien, B. Shokri and M. Kharazi, Synergism in mixtures of nano benzimidazolium Gemini ionic liquid and sodium dodecyl sulfate surfactants in tuning interfacial properties of crude oil-water system, *J. Mol. Liq.*, 2023, **391**, 123280, DOI: [10.1016/j.molliq.2023.123280](https://doi.org/10.1016/j.molliq.2023.123280).



15 S. Asadabadi, J. Saien and M. Kharazi, Enhanced interfacial activity by maximizing synergy between long-chain ionic liquid and conventional surfactant for enhanced oil recovery, *RSC Adv.*, 2024, **14**, 18942–18949, DOI: [10.1039/D4ra02092h](https://doi.org/10.1039/D4ra02092h).

16 J. Saien, A. Eghetenaei and M. Kharazi, Qualifying interfacial properties of crude oil–water system with the synergistic action of a nano Gemini ionic liquid and conventional surfactants, *Sci. Rep.*, 2024, **14**, 19833, DOI: [10.1038/s41598-024-70888-4](https://doi.org/10.1038/s41598-024-70888-4).

17 A. Dan, R. Wüstneck, J. Krägel, E. V. Aksenenko, V. B. Fainerman and R. Miller, Interfacial adsorption and rheological behavior of β -casein at the water/hexane interface at different pH, *Food Hydrocoll.*, 2014, **34**, 193–201, DOI: [10.1016/j.foodhyd.2012.10.015](https://doi.org/10.1016/j.foodhyd.2012.10.015).

18 J. Saien and S. Asadabadi, Alkyl chain length, counter anion and temperature effects on the interfacial activity of imidazolium ionic liquids: comparison with structurally related surfactants, *Fluid Phase Equilib.*, 2015, **386**, 134–139, DOI: [10.1016/j.fluid.2014.12.002](https://doi.org/10.1016/j.fluid.2014.12.002).

19 M. Kharazi, J. Saien, M. Torabi and M. A. Zolfigol, Green nano multicationic ionic liquid based surfactants for enhanced oil recovery: a comparative study on design and applications, *J. Mol. Liq.*, 2023, **383**, 122090, DOI: [10.1016/j.molliq.2023.122090](https://doi.org/10.1016/j.molliq.2023.122090).

20 D. Štanfel, L. Kalogjera, S. V. Ryazantsev, K. Hlača, E. Y. Radtsig, R. Teimuraz and P. Hrabač, The role of seawater and saline solutions in treatment of upper respiratory conditions, *Mar. Drugs*, 2022, **20**, 330, DOI: [10.3390/md20050330](https://doi.org/10.3390/md20050330).

21 M. Lan, X. Wang, P. Chen and X. Zhao, Effects of surface tension and wood surface roughness on impact splash of a pure and multi-component water drop, *Case Stud. Therm. Eng.*, 2016, **8**, 218–225, DOI: [10.1016/j.csite.2016.07.006](https://doi.org/10.1016/j.csite.2016.07.006).

22 A. Kakati and J. S. Sangwai, Effect of monovalent and divalent salts on the interfacial tension of pure hydrocarbon-brine systems relevant for low salinity water flooding, *J. Pet. Sci. Eng.*, 2017, **157**, 1106–1114, DOI: [10.1016/j.petrol.2017.08.017](https://doi.org/10.1016/j.petrol.2017.08.017).

23 B. Gao and M. M. Sharma, A family of alkyl sulfate gemini surfactants. 2. Water–oil interfacial tension reduction, *J. Colloid Interface Sci.*, 2013, **407**, 375–381, DOI: [10.1016/j.jcis.2013.04.043](https://doi.org/10.1016/j.jcis.2013.04.043).

24 H. Zhou, Y. Liang, P. Huang, T. Liang, H. Wu, P. Lian, X. Leng, C. Jia, Y. Zhu and H. Jia, Systematic investigation of ionic liquid-type gemini surfactants and their abnormal salt effects on the interfacial tension of a water/model oil system, *J. Mol. Liq.*, 2018, **249**, 33–39, DOI: [10.1016/j.molliq.2017.11.004](https://doi.org/10.1016/j.molliq.2017.11.004).

25 Y. F. Yano, T. Uruga, H. Tanida, Y. Terada and H. Yamada, Protein salting out observed at an air–water interface, *J. Phys. Chem. Lett.*, 2011, **2**, 995–999, DOI: [10.1021/jz200111q](https://doi.org/10.1021/jz200111q).

26 R. Borwankar and D. Wasan, Equilibrium and dynamics of adsorption of surfactants at fluid–fluid interfaces, *Chem. Eng. Sci.*, 1988, **43**, 1323–1337, DOI: [10.1016/0009-2509\(88\)85106-6](https://doi.org/10.1016/0009-2509(88)85106-6).

27 R. Zimmermann, U. Freudenberg, R. Schweiß, D. Küttner and C. Werner, Hydroxide and hydronium ion adsorption—a survey, *Curr. Opin. Colloid Interface Sci.*, 2010, **15**, 196–202, DOI: [10.1016/j.cocis.2010.01.002](https://doi.org/10.1016/j.cocis.2010.01.002).

28 L. He, F. Lin, X. Li, H. Sui and Z. Xu, Interfacial sciences in unconventional petroleum production: from fundamentals to applications, *Chem. Soc. Rev.*, 2015, **44**, 5446–5494, DOI: [10.1039/c5cs00102a](https://doi.org/10.1039/c5cs00102a).

29 J. Saien, M. Kharazi, *Properties and Applications of Surface-active Ionic Liquids*, Nova Science, 2023, DOI: [10.52305/HFEO4188](https://doi.org/10.52305/HFEO4188).

30 B. Dong, N. Li, L. Zheng, L. Yu and T. Inoue, Surface adsorption and micelle formation of surface active ionic liquids in aqueous solution, *Langmuir*, 2007, **23**, 4178–4182, DOI: [10.1021/la0633029](https://doi.org/10.1021/la0633029).

31 H. Kumar and G. Kaur, Scrutinizing Self-Assembly, Surface Activity and Aggregation Behavior of Mixtures of Imidazolium Based Ionic Liquids and Surfactants: A Comprehensive Review, *Front. Chem.*, 2021, **9**, 667941, DOI: [10.3389/fchem.2021.667941](https://doi.org/10.3389/fchem.2021.667941).

32 G. Liu, D. Gu, H. Liu, W. Ding, H. Luan and Y. Lou, Thermodynamic properties of micellization of Sulfolobetaine-type Zwitterionic Gemini Surfactants in aqueous solutions – a free energy perturbation study, *J. Colloid Interface Sci.*, 2012, **375**, 148–153, DOI: [10.1016/j.jcis.2012.02.027](https://doi.org/10.1016/j.jcis.2012.02.027).

33 C. S. Buettner, A. Cognigni, C. Schröder and K. Bica-Schröder, Surface-active ionic liquids: a review, *J. Mol. Liq.*, 2022, **347**, 118160, DOI: [10.1016/j.molliq.2021.118160](https://doi.org/10.1016/j.molliq.2021.118160).

34 R. Kumari, A. Kakati, R. Nagarajan and J. S. Sangwai, Synergistic effect of mixed anionic and cationic surfactant systems on the interfacial tension of crude oil–water and enhanced oil recovery, *J. Dispersion Sci. Technol.*, 2018, **40**, 969–981, DOI: [10.1080/01932691.2018.1489280](https://doi.org/10.1080/01932691.2018.1489280).

35 Y. Xu, T. Wang, L. Zhang, Y. Tang, W. Huang and H. Jia, Investigation on the effects of cationic surface active ionic liquid/anionic surfactant mixtures on the interfacial tension of water/crude oil system and their application in enhancing crude oil recovery, *J. Dispersion Sci. Technol.*, 2021, **44**, 214–224, DOI: [10.1080/01932691.2021.1942034](https://doi.org/10.1080/01932691.2021.1942034).

36 J. Saien, B. Shokri and M. Kharazi, Effective synergistic action of benzimidazolium nano gemini ionic liquid and conventional surfactant for chemical enhanced oil recovery, *ACS Omega*, 2024, **9**, 22336–22344, DOI: [10.1021/acsomega.4c01768](https://doi.org/10.1021/acsomega.4c01768).

37 S. Chowdhury, S. Shrivastava, A. Kakati and J. S. Sangwai, Comprehensive review on the role of surfactants in the chemical enhanced oil recovery process, *Ind. Eng. Chem. Res.*, 2022, **61**, 21–64, DOI: [10.1021/acs.iecr.1c03301](https://doi.org/10.1021/acs.iecr.1c03301).

38 S. Pal, M. Mushtaq, F. Banat and A. M. Al Sumaiti, Review of surfactant-assisted chemical enhanced oil recovery for carbonate reservoirs: challenges and future perspectives, *Pet. Sci.*, 2017, **15**, 77–102, DOI: [10.1007/s12182-017-0198-6](https://doi.org/10.1007/s12182-017-0198-6).

39 S. K. Nandwani, M. Chakraborty, H.-J. Bart and S. Gupta, Synergism, phase behaviour and characterization of ionic liquid–nonionic surfactant mixture in high salinity



environment of oil reservoirs, *Fuel*, 2018, **229**, 167–179, DOI: [10.1016/j.fuel.2018.05.021](https://doi.org/10.1016/j.fuel.2018.05.021).

40 H. Jia, P. Lian, X. Leng, Y. Han, Q. Wang, K. Jia, X. Niu, M. Guo, H. Yan and K. Lv, Mechanism studies on the application of the mixed cationic/anionic surfactant systems to enhance oil recovery, *Fuel*, 2019, **258**, 116156–116165, DOI: [10.1016/j.fuel.2019.116156](https://doi.org/10.1016/j.fuel.2019.116156).

41 M. U. H. Shah, M. Moniruzzaman, M. Sivapragasam, M. M. R. Talukder, S. B. Yusup and M. Goto, A binary mixture of a biosurfactant and an ionic liquid surfactant as a green dispersant for oil spill remediation, *J. Mol. Liq.*, 2019, **280**, 111–119, DOI: [10.1016/j.molliq.2019.02.049](https://doi.org/10.1016/j.molliq.2019.02.049).

42 M. Nazar, M. U. H. Shah, W. Z. N. Yahya, M. Goto and M. Moniruzzaman, Surface active ionic liquid and Tween-80 blend as an effective dispersant for crude oil spill remediation, *Environ. Technol. Innovation*, 2021, **24**, 101868–101881, DOI: [10.1016/j.eti.2021.101868](https://doi.org/10.1016/j.eti.2021.101868).

43 A. F. Olea and C. Gamboa, Synergism in mixtures of cationic surfactant and anionic copolymers, *J. Colloid Interface Sci.*, 2003, **257**, 321–326, DOI: [10.1016/s0021-9797\(02\)00019-x](https://doi.org/10.1016/s0021-9797(02)00019-x).

